PCCP

PAPER

View Article Online
View Journal | View Issue

Cite this: *Phys. Chem. Chem. Phys.*, 2014, **16**, 24417

The $KCaSrTa_5O_{15}$ photocatalyst with tungsten bronze structure for water splitting and CO_2 reduction†

Tomoaki Takayama,[a] Kentaro Tanabe,[a] Kenji Saito,‡[a] Akihide Iwase[ab] and Akihiko Kudo*[ab]

Received 29th August 2014,
Accepted 1st October 2014

DOI: 10.1039/c4cp03892d

www.rsc.org/pccp

$KCaSrTa_5O_{15}$ with tungsten bronze structure and a band gap of 4.1 eV showed activity for water splitting without cocatalysts. The activity was improved by loading the NiO cocatalyst. The apparent quantum yield of optimized NiO-loaded $KCaSrTa_5O_{15}$ was 2.3% at 254 nm for water splitting. When CO_2 gas was bubbled into the reactant aqueous solution, Ag cocatalyst-loaded $KCaSrTa_5O_{15}$ produced CO and H_2 as reduction products of CO_2 and H_2O, respectively, and O_2 as an oxidation product of H_2O. The carbon source of CO was confirmed to be CO_2 molecules by using $^{13}CO_2$. The ratio of the number of electrons to that of holes calculated from the amounts of products (CO, H_2 and O_2) was almost unity. Additionally, the ratio of the turnover number of electrons consumed for CO production to the total number of an Ag atom of the cocatalyst that was the active site for CO_2 reduction was 8.6 at 20 h. These results indicate that water was consumed as an electron donor for this photocatalytic CO_2 reduction in an aqueous medium. Thus, $KCaSrTa_5O_{15}$ with tungsten bronze structure has arisen as a new photocatalyst that is active for water splitting and CO_2 reduction utilizing water as an electron donor.

Introduction

An artificial photosynthesis system has been extensively studied to develop systems for CO_2 conversion to fuels and chemicals. Photocatalytic CO_2 reduction is one of the potential candidates for the artificial photosynthesis. Homogeneous and heterogeneous photocatalyst systems for CO_2 reduction have been studied. The homogeneous photocatalysts including Re-complex and Re–Ru-complex require sacrificial reducing reagents such as TEOA (Triethanolamine) to reduce CO_2 to CO and HCOOH.[1–6] Although a heterogeneous CdS photocatalyst shows activity for CO_2 reduction to form CO under visible light irradiation, sacrificial reagents are also indispensable.[7,8] Heterogeneous metal oxide photocatalysts which possess the ability for O_2 evolution by oxidation of water have been reported for the CO_2 reduction to form HCOOH, CO, CH_3OH and CH_4 in aqueous media without sacrificial reagents.[9–16] However, oxygen evolution in a stoichiometric amount is not observed in many cases. Among them, a ZrO_2 photocatalyst produces CO and H_2 as reduction products and O_2 as an oxidation product in a stoichiometric amount under UV light irradiation.[14] Moreover, the selectivity for CO_2 reduction to form CO are enhanced by loading a Cu cocatalyst on the ZrO_2 photocatalyst. $BaLa_4Ti_4O_{15}$[15] and Zn-doped Ga_2O_3[16] are highly active for CO_2 reduction using water as an electron donor when Ag cocatalyst is employed. Thus, metal oxide photocatalysts for water splitting can be applied to CO_2 reduction using water as an electron donor if suitable cocatalysts are chosen.

We have developed tantalum-based photocatalysts, such as $NaTaO_3$ and $NaTaO_3$:A (A = La and Sr) with perovskite structure, and $K_2LnTa_5O_{15}$ (Ln = La, Pr, Nd, Sm, Gd, Tb, Dy and Tm) with tungsten bronze structure, for highly efficient water splitting under UV light irradiation.[17–19] The high activities for the tantalum-based photocatalysts are mainly due to their high conduction bands formed by Ta 5d orbitals. We have also reported that a $BaLa_4Ti_4O_{15}$ photocatalyst[20] with two dimensional anisotropy of crystal structure for water splitting also shows activity for CO_2 reduction using water as an electron donor by loading a highly dispersed Ag cocatalyst.[15] The selectivity for the CO_2 reduction is superior to that for water reduction to form H_2 even in an aqueous medium. On the other

[a] *Department of Applied Chemistry, Faculty of Science, Tokyo University of Science, 1-3 Kagurazaka, Shinjuku-ku, Tokyo, 162-8601, Japan. E-mail: a-kudo@rs.kagu.tus.ac.jp; Fax: +81-3-5261-4631*

[b] *Photocatalysis International Research Center, Research Institute for Science and Technology, Tokyo University of Science, 2641 Yamazaki, Noda-shi, Chiba, 278-8510, Japan*

† Electronic supplementary information (ESI) available. See DOI: 10.1039/c4cp03892d

‡ Present address: Office for Development of Young Researchers, Research Planning and Promotion Division, Niigata University, 8050 Ikarashi 2-no-cho, Nishi-ku, Niigata 950-2181, Japan.

hand, there is a tantalate group that possesses tungsten bronze structure with anisotropy to a *c*-axis of the crystal structure and the framework consisting of TaO_6 octahedra with corner sharing being similar to the perovskite structure as seen in $NaTaO_3$ of a highly efficient photocatalyst for water splitting. Therefore, the tantalates with tungsten bronze structure are expected to be active for water splitting and CO_2 reduction. In the present study, $KCaSrTa_5O_{15}$ with tungsten bronze structure[21] was prepared using a solid-state reaction, and their photocatalytic activities for water splitting and CO_2 reduction were investigated. The photocatalyst particles and cocatalysts were characterized using SEM, XPS and DRS.

Experimental

Preparation of $KCaSrTa_5O_{15}$

$KCaSrTa_5O_{15}$ was prepared by a solid-state reaction as follows. K_2CO_3 (Kanto Chemical: 99.0%), $CaCO_3$ (Kanto Chemical: 99.5%), $SrCO_3$ (Kanto Chemical: 99.9%) and Ta_2O_5 (Rare Metallic: 99.99%) were used as starting materials for the solid-state reaction. The carbonates and oxide were mixed in a molar ratio of K : Ca : Sr : Ta = 1.05 : 1 : 1 : 5 in an alumina mortar. The excess amount of potassium (5 mol%) was to compensate the volatilization.[22] The mixed powder was calcined in air at 1173 K for 1 h and subsequently at 1423 K for 10 h in a platinum crucible. The excess potassium was washed out with water from the obtained powder.

Various cocatalysts were loaded by impregnation and photodeposition methods on the surface of the $KCaSrTa_5O_{15}$ photocatalyst. NiO and Ag cocatalysts were loaded by an impregnation method. Photocatalyst powder was dispersed in aqueous solutions to dissolve $Ni(NO_3)_2$ (Wako Pure Chemical: 98.5%) and $AgNO_3$ (Tanaka Rare Metal) in a porcelain crucible. The slurry solution was stirred with a glass rod during evaporation using a hot plate. The obtained powder was calcined in air at 575 K and 723 K for 1 h for loading the NiO and Ag cocatalysts, respectively. The NiO and Ag cocatalysts were reduced with H_2 at 773 K, if necessary. Ag, Ni, Ru, Rh, Pt, Cu and Au cocatalysts were photodeposited from aqueous solutions to dissolve suitable amounts of $AgNO_3$, $Ni(NO_3)_2$, $RuCl_3$, $RhCl_3$, H_2PtCl_6, $Cu(NO_3)_2$ and $HAuCl_4$ *in situ*.

$KCaSrTa_5O_{15}$ powders prepared by a solid-state reaction at different temperatures were examined by X-ray diffraction using Cu Kα radiation (Rigaku: Miniflex). Diffuse reflectance spectra of these powders were recorded using a UV-vis-NIR spectrometer (Jasco: UbestV-570) and were converted from reflection to absorption by the Kubelka–Munk method. Photocatalyst powders were observed using a scanning electron microscope (JEOL: JSM-6700F). Surface species of cocatalysts on photocatalysts were analyzed by X-ray photoelectron spectroscopy (Shimazdu: ESCA-3400; Mg anode). Metallic Ni (Nilaco: 99+%), NiO (Soekawa Chemical: 99.9%) and $Ni(OH)_2$ (Wako Pure Chemical: 95.0%) were employed as references for the XPS measurements. Binding energies were corrected using C 1s (285.0 eV) on a metallic Au foil (84.0 eV).[23]

Photocatalytic water splitting and CO_2 reduction

Photocatalytic reactions were conducted using an inner irradiation cell made of quartz with a 400 W high-pressure mercury lamp. 0.5 g of photocatalyst powder was dispersed in 350 mL of water. The Ar (99.99%) or CO_2 (99.995%) gas was continuously bubbled at a 30 mL min^{-1} flow rate during the photocatalytic reaction. Gaseous products of H_2, O_2 and CO were determined by GC (Shimadzu: GC-8A with Molecular Sieve 5A, TCD and Ar carrier, and GC-8A with methanizer, Molecular Sieve 13X, FID and N_2 carrier). $^{13}CO_2$ (purity: 99.5 atom%) was also employed for an isotope experiment to confirm the carbon source for photocatalytic CO_2 reduction. ^{13}CO was analyzed using a GC-MS (Shimadzu: GC-MS Plus 2010, RESTEK: RT-Msieve 5A).

Results and discussion

Characterization of $KCaSrTa_5O_{15}$

The X-ray diffraction patterns of the materials prepared at different calcination temperatures were assigned to $KCaSrTa_5O_{15}$ (PDF: 40-351) (Fig. S1, ESI†). Calcination below 1573 K gave small amounts of $Ca_2Ta_2O_7$ (PDF: 53-743) and an unknown compound as impurities (Fig. S1 (a)–(c), ESI†), while the single phase of highly crystalline $KCaSrTa_5O_{15}$ was obtained by calcining at 1773 K for 10 h (Fig. S1(d), ESI†). The band gap of $KCaSrTa_5O_{15}$ was estimated to be 4.1 eV from the absorption edges except for the material prepared at 1173 K as shown in Fig. 1. Primary particles of $KCaSrTa_5O_{15}$ with an average diameter of 200–300 nm aggregated, when they were prepared below 1573 K as shown in Fig. 2(a)–(c). In contrast, the morphology of $KCaSrTa_5O_{15}$ prepared at 1773 K was a rod as shown in Fig. 2(d), reflecting the tungsten bronze structure in which TaO_6 octahedral units were connected to each other along the *c*-axis.

Effect of loading the cocatalyst on water splitting and CO_2 reduction

Table 1 shows the activity for water splitting over $KCaSrTa_5O_{15}$ under Ar gas flow. All samples prepared at different temperatures showed the activity for water splitting without a cocatalyst. Moreover, the activities were drastically enhanced when the NiO

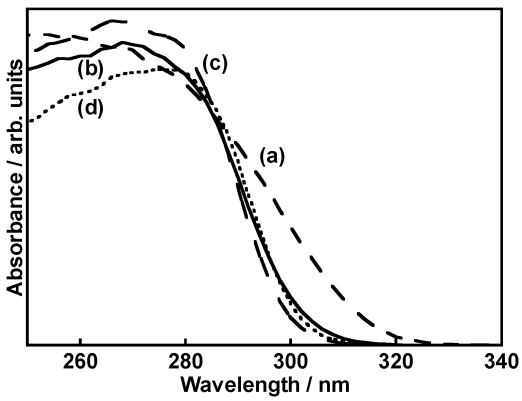

Fig. 1 Diffuse reflectance spectra of $KCaSrTa_5O_{15}$ prepared at (a) 1173 K, (b) 1423 K, (c) 1573 K and (d) 1773 K for 10 h.

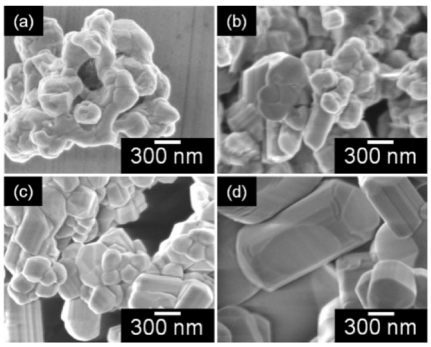

Fig. 2 SEM images of $KCaSrTa_5O_{15}$ prepared at (a) 1173 K, (b) 1423 K, (c) 1573 K and (d) 1773 K for 10 h.

Table 1 Photocatalytic water splitting over $KCaSrTa_5O_{15}$ prepared at different temperatures

Preparation temperature/K	Cocatalyst	Loading method	Activity/μmol h^{-1}	
			H_2	O_2
1173	None	—	271	180
1173	NiO	Impregnation	639	263
1423	None	—	102	42
1423	NiO	Impregnation	1339	700
1423	Ni	Photodeposition	25	12
1423	Ni	Impregnation + H_2 red.	115	62
1573	None	—	106	47
1573	NiO	Impregnation	1270	644
1773	None	—	66	31
1773	NiO	Impregnation	212	95

Photocatalyst: 0.5 g, cocatalyst: 0.5 wt%, loading conditions: impregnation (573 K for 1 h in air), impregnation and subsequent H_2 reduction (773 K for 2 h in H_2 flow), photodeposition (*in situ*), reactant solution: water (350 mL), light source: a 400 W high-pressure mercury lamp, reactor: an inner irradiation cell made of quartz. $KCaSrTa_5O_{15}$ was prepared by a solid-state reaction.

cocatalyst was loaded on $KCaSrTa_5O_{15}$. In contrast, the activities of $KCaSrTa_5O_{15}$ were not enhanced when Ni cocatalysts were loaded by photodeposition, and impregnation and H_2 reduction. NiO-loaded $KCaSrTa_5O_{15}$ prepared at 1423 K showed the highest activity. Although the initial activity of this photocatalyst was high, the rates of H_2 and O_2 evolution decreased at the initial stage as shown in Fig. 3. H_2 and O_2 steadily evolved in a stoichiometric amount after the deactivation. The apparent quantum yield was 2.3% at 254 nm for water splitting (Fig. S2, ESI†). Thus, $KCaSrTa_5O_{15}$ with tungsten bronze structure has arisen as a new photocatalyst for water splitting.

The $KCaSrTa_5O_{15}$ photocatalyst was applied to CO_2 reduction as shown in Table 2. The pristine $KCaSrTa_5O_{15}$ produced only H_2 and O_2 without any reduction products of CO_2. This indicates that there were no active sites for CO_2 reduction on the surface of the $KCaSrTa_5O_{15}$ photocatalyst. Therefore, various cocatalysts were loaded to introduce active sites. Water splitting activity of $KCaSrTa_5O_{15}$ was enhanced when effective cocatalysts such as NiO and Au[17,24,25] for water splitting were loaded as observed for the $BaLa_4Ti_4O_{15}$ photocatalyst.[15] No CO_2 reduction proceeded, when Ni, Ru, Rh, Pd, Pt and Au were loaded. When the Cu cocatalyst was loaded, a small amount of CO evolved. In contrast,

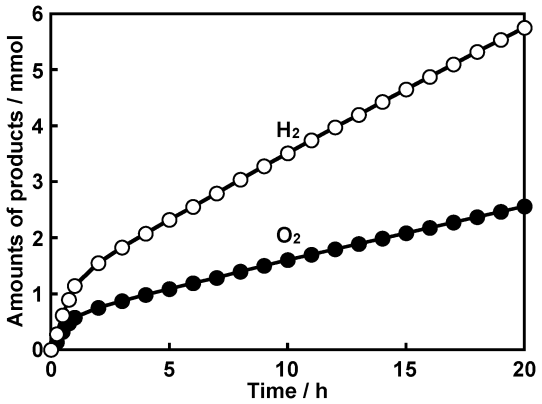

Fig. 3 Water splitting over NiO (0.5 wt%)-loaded $KCaSrTa_5O_{15}$ photocatalyst. Photocatalyst: 0.5 g, reactant solution: water (350 mL) with Ar gas flow (30 mL min^{-1}), light source: a 400 W high-pressure mercury lamp, reactor: an inner irradiation cell made of quartz. $KCaSrTa_5O_{15}$ was prepared by a solid-state reaction at 1423 K for 10 h. The NiO cocatalyst was loaded by an impregnation method.

Table 2 Photocatalytic CO_2 reduction over various cocatalysts-loaded $KCaSrTa_5O_{15}$

Cocatalyst	Loading condition	Activity/μmol h^{-1}		
		H_2	O_2	CO
None	—	116	48	0
NiO	Impregnation[a]	764	398	0
Ni	Photodeposition	111	58	0
Cu	Photodeposition	216	100	Trace
Ru	Photodeposition	28	13	0
Rh	Photodeposition	43	19	0
Ag	Photodeposition	53	37	8.1
Ag	Impregnation[b]	55	28	5.5
Ag	Impregnation[b] + H_2 red.	96	48	1.0
Pt	Photodeposition	62	23	0
Au	Photodeposition	584	269	0

Photocatalyst: 0.5 g, cocatalysts: 0.5 wt%, loading conditions: photodeposition (*in situ*), impregnation ([a] 573 K for 1 h in air, [b] 723 K for 1 h in air), impregnation and subsequent H_2 reduction (773 K for 2 h in H_2 flow), reactant solution: CO_2 dissolved in water (350 mL) under 1 atm, light source: a 400 W high-pressure mercury lamp, reactor: an inner irradiation cell made of quartz. $KCaSrTa_5O_{15}$ was prepared by a solid-state reaction at 1423 K for 10 h.

the Ag-loaded $KCaSrTa_5O_{15}$ photocatalyst produced CO from CO_2 as a reduction product regardless of loading methods of the Ag cocatalyst. In particular, the high activity for CO_2 reduction was observed, when the Ag cocatalyst was loaded by photodeposition and impregnation methods as shown in Table 2 and Fig. S3 (ESI†). The fact that CO_2 was reduced on the Ag-loaded $KCaSrTa_5O_{15}$, but not on the pristine $KCaSrTa_5O_{15}$, indicates that the Ag cocatalyst works as a reduction site for CO_2. Metallic Ag is a good electrocatalyst for reduction of CO_2 to CO.[26] The process of CO_2 reduction to CO on the Ag cocatalyst would be similar to that on the Ag electrocatalyst[27,28] as observed for $BaLa_4Ti_4O_{15}$[15] and Zn-doped Ga_2O_3[16] photocatalysts. A CO_2 molecule is reduced to $CO_2^{\bullet-}$ adsorbed on a Ag cocatalyst by a photoexcited electron. Although the redox potential of $CO_2^{\bullet-}$ formation is −1.9 V,[27] the redox potential should become more

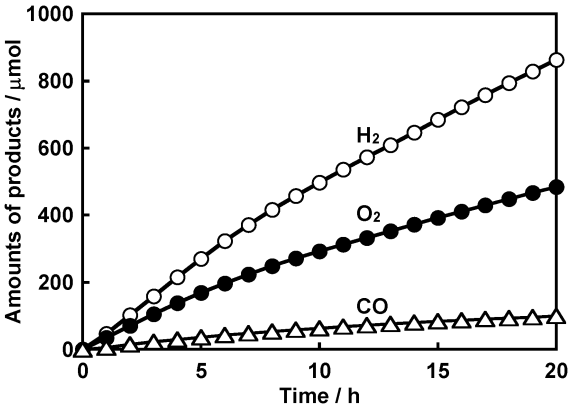

Fig. 4 CO_2 reduction over Ag (0.5 wt%)-loaded $KCaSrTa_5O_{15}$ photocatalyst in an aqueous medium. Photocatalyst: 0.5 g, reactant solution: water (350 mL) with CO_2 gas flow (30 mL min^{-1}), light source: a 400 W high-pressure mercury lamp, reactor: an inner irradiation cell made of quartz. $KCaSrTa_5O_{15}$ was prepared by a solid-state reaction at 1423 K for 10 h. The Ag cocatalyst was loaded by a photodeposition.

positive due to stabilization by adsorption. The adsorbed $CO_2^{\bullet -}$ is reacted with a H^+ ion in water to form an adsorbed –COOH. The adsorbed –COOH is subsequently reduced to become CO and OH^- by another electron.[27,28]

H_2, O_2 and CO evolved steadily with a reaction time on the optimized Ag-loaded $KCaSrTa_5O_{15}$ photocatalyst as shown in Fig. 4. The turnover number of electrons reacted for CO evolution to the number of the Ag atoms in the cocatalyst calculated using eqn (1) was 8.6 at 20 h, and the ratio of electrons to holes calculated using eqn (2) was unity. These results indicate that the CO_2 reduction over Ag-loaded $KCaSrTa_5O_{15}$ proceeded photocatalytically and water was used as an electron donor.

$$TON_{CO_2} = (\text{The number of electrons consumed for CO formation})/(\text{The total number of a Ag atom in cocatalyst on } KCaSrTa_5O_{15}) \quad (1)$$

$$e^-/h^+ = (\text{The number of electrons consumed for } H_2 \text{ and CO formation})/(\text{The numbers of holes consumed for } O_2 \text{ formation}) \quad (2)$$

It has been reported that methane forms from not CO_2 but an organic contamination adsorbed on the photocatalyst surface.[29] Therefore, an isotope experiment using $^{13}CO_2$ was carried out to clarify the carbon source of CO formed. When the $^{13}CO_2$ gas was analyzed using a GC-MS and using a MS-5A column, no peaks due to ^{12}CO and ^{13}CO were detected, indicating that the $^{13}CO_2$ gas contained negligible amounts of ^{12}CO and ^{13}CO. In contrast, photocatalytic reduction of $^{13}CO_2$ over Ag-loaded $KCaSrTa_5O_{15}$ photocatalyst gave ^{13}CO and not ^{12}CO (Fig. S4, ESI†). Additionally, the ratio of electrons to holes calculated from the products was about unity also in this isotopic experiment. Therefore, it was proven that CO was produced from CO_2 molecules over the Ag-loaded $KCaSrTa_5O_{15}$ photocatalyst.

Characterization of cocatalysts loaded on $KCaSrTa_5O_{15}$

NiO and Ag cocatalysts loaded on $KCaSrTa_5O_{15}$ before and after photocatalytic water splitting and CO_2 reduction were analyzed by scanning electron microscopy (SEM), X-ray photoelectron spectroscopy (XPS) and diffuse reflectance spectroscopy (DRS) in order to clarify the active states of these cocatalysts.

The particle size and morphology of NiO and Ni cocatalysts loaded on $KCaSrTa_5O_{15}$ photocatalysts were observed using SEM before and after photocatalytic water splitting (Fig. S5, ESI†). The particle size of NiO loaded by an impregnation method was about 10 nm (Fig. S5(a), ESI†). Small particle sizes of metallic Ni remained after H_2 reduction, though a part of metallic Ni sintered (Fig. S5(c), ESI†). The metallic Ni aggregated after the photocatalytic water splitting, and nanoparticles of Ni were hardly observed (Fig. S5(d), ESI†). The shape of Ni loaded by a photodeposition method was not spherical being clearly different from that loaded by an impregnation method (Fig. S5(e), ESI†). Thus, the particle size and the shape of NiO and/or Ni cocatalysts after photocatalytic water splitting depended on the loading methods.

Fig. 5 shows DRS of NiO and Ni-loaded $KCaSrTa_5O_{15}$ before and after photocatalytic water splitting. Non-loaded $KCaSrTa_5O_{15}$ was white and possessed 302 nm of an absorption edge (Fig. 5(a)). A color of $KCaSrTa_5O_{15}$ loaded with NiO by an impregnation method was gray and the background of the DRS arose at visible and near IR regions (Fig. 5(b)). A color of $Ni/KCaSrTa_5O_{15}$ obtained by an impregnation and subsequent H_2 reduction was pale brown and gave a broad absorption band with a peak at around 400 nm (Fig. 5(d)). All Ni or NiO-loaded photocatalysts were dark purple after photocatalytic water splitting giving broad absorption bands in the visible light region (Fig. 5(c), (e) and (f)). These results suggest that the condition of nickel cocatalysts was similar to each other during photocatalytic water splitting regardless of the loading methods.

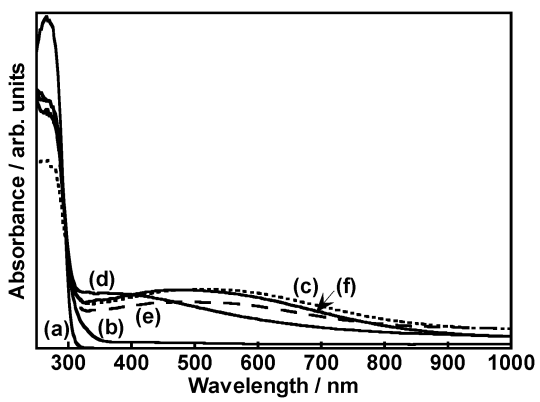

Fig. 5 Diffuse reflectance spectra of (a) pristine $KCaSrTa_5O_{15}$ and (b)–(f) NiO (0.5 wt%) and Ni (0.5 wt%)-loaded $KCaSrTa_5O_{15}$ by various methods before and after water splitting. (b) Before and (c) after water splitting for the samples prepared by an impregnation method, (d) before and (e) after water splitting for the samples prepared by impregnation and subsequent H_2 reduction, (f) after water splitting for the samples prepared by a photodeposition. $KCaSrTa_5O_{15}$ was prepared by a solid-state reaction at 1423 K for 10 h.

The dark purple color did not quickly change after being exposed to air.

Fig. 6 shows XPS of Ni 2p of NiO and Ni cocatalysts loaded on $KCaSrTa_5O_{15}$ before and after photocatalytic water splitting. Binding energies of standard samples of metallic Ni, NiO and $Ni(OH)_2$ agreed with those of previous reports.[30] The surface of the standard NiO powder was covered with surface hydroxyl groups. NiO loaded on $KCaSrTa_5O_{15}$ by an impregnation method also gave peaks due to NiO and $Ni(OH)_2$ (Fig. 6(a)). $Ni/KCaSrTa_5O_{15}$ obtained by an impregnation and subsequent H_2 reduction gave XPS signals due to metallic Ni with NiO (Fig. 6(c)). All samples showed XPS signals mainly due to $Ni(OH)_2$ after photocatalytic water splitting (Fig. 6(b), (d) and (e)). $Ni(OH)_2$ is generally green, not dark purple as mentioned above. DRS of the samples after photocatalytic water splitting was different from that of $Ni(OH)_2$ (Fig. S6, ESI†). Therefore, the XPS signals due to $Ni(OH)_2$ observed for the samples after photocatalytic water splitting indicate the existence of not bulky $Ni(OH)_2$ but the surface nickel hydroxide as observed for a $NiO_x/SrTiO_3$ photocatalyst.[30] It has been reported that the color of the $NiO/InBO_4$ photocatalyst also changed to dark purple after photocatalytic water splitting.[31] An ultra fine NiO cocatalyst loaded on a $NaTaO_3$:La photocatalyst gives visible light absorption bands which are different from that of $Ni(OH)_2$.[32] Thus, an active NiO cocatalyst loaded on the photocatalysts with wide band gaps has a unique character.

The impregnation method for loading the nickel cocatalyst was more effective than impregnation and subsequent H_2 reduction, and photodeposition methods for water splitting over the $KCaSrTa_5O_{15}$ photocatalyst as shown in Table 1. SEM and XPS measurements suggested that most active $KCaSrTa_5O_{15}$ photocatalysts possessed the cocatalyst of fine NiO particles covered with surface nickel hydroxide.

SEM images of Ag loaded $KCaSrTa_5O_{15}$ photocatalysts were also observed before and after photocatalytic CO_2 reduction (Fig. S7, ESI†). The impregnation method gave a Ag cocatalyst with a particle size of about 10 nm before and after H_2 reduction (Fig. S7(a) and (c), ESI†). The Ag cocatalyst aggregated after photocatalytic CO_2 reduction (Fig. S7(b) and (d), ESI†). The growth of some Ag particles reached up to 50–100 nm. The particle size of Ag after photocatalytic CO_2 reduction was similar to that obtained by a photodeposition method (Fig. S7(e) and (f), ESI†).

Nano-sized metallic Ag particles generally give a surface plasmonic absorption band in visible light region.[33] Therefore, DRS of samples before and after photocatalytic CO_2 reduction was obtained as shown in Fig. 7. The Ag cocatalyst obtained by H_2 reduction was orange in color and gave a characteristic surface plasmonic absorption spectrum (Fig. 7(c)), while such a spectrum was not observed for the Ag cocatalyst obtained by the impregnation method (Fig. 7(a)). All samples after photocatalytic CO_2 reduction gave similar absorption spectra to the sample obtained by H_2 reduction (Fig. 7(b), (d), (e) and (f)), although the intensities of the absorption spectra decreased after the photocatalytic reduction of CO_2. These results suggest dissolution and re-deposition of Ag during the photocatalytic reaction giving aggregated Ag particles as observed by SEM. The Ag cocatalyst prepared by the impregnation method after the photocatalytic reduction of CO_2 also gave the similar absorption spectrum

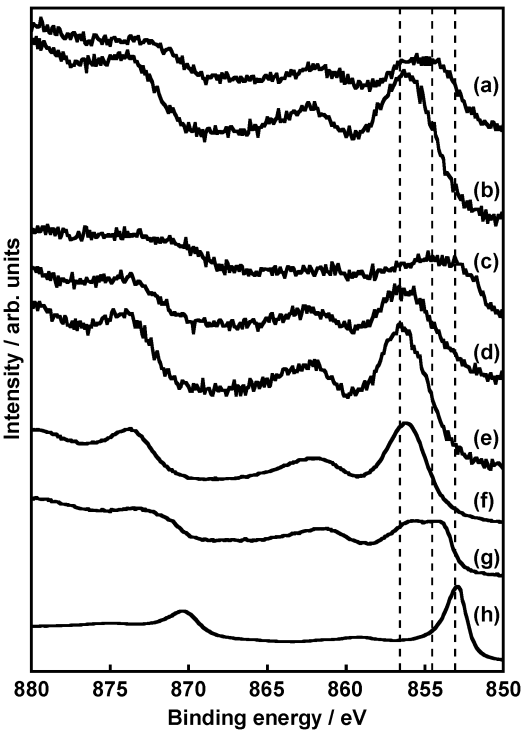

Fig. 6 X-ray photoelectron spectra of Ni 2p of NiO (0.5 wt%) and Ni (0.5 wt%)-loaded $KCaSrTa_5O_{15}$. (a) before and (b) after water splitting for the samples prepared by an impregnation method, (c) before and (d) after water splitting for the samples prepared by an impregnation and subsequent H_2 reduction, (e) after water splitting for the sample prepared by a photodeposition. Standard sample of (f) $Ni(OH)_2$, (g) NiO, (h) metallic Ni foil. Reference data[30] are indicated as dashed lines respectively: Ni metal (853.1 eV), NiO (854.5 eV), $Ni(OH)_2$ (856.6 eV).

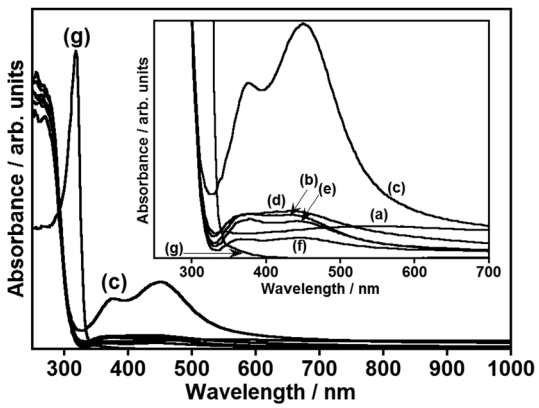

Fig. 7 Diffuse reflectance spectra of Ag (0.5 wt%)-loaded $KCaSrTa_5O_{15}$ by various methods before and after CO_2 reduction. (a) Before and (b) after CO_2 reduction for the samples prepared by an impregnation method, (c) before and (d) after CO_2 reduction for the samples prepared by an impregnation and subsequent H_2 reduction, after CO_2 reduction for the samples prepared by a photodeposition at (e) 2 h and (f) 20 h, and (g) metallic and bulky Ag. $KCaSrTa_5O_{15}$ was prepared by a solid-state reaction at 1423 K for 10 h.

indicating that the Ag cocatalyst was reduced to fine metallic particles by photogenerated electrons. These results indicate that the metallic Ag giving the surface plasmonic absorption spectrum is an active site for the photocatalytic CO_2 reduction.

Conclusions

$KCaSrTa_5O_{15}$ (BG = 4.1 eV) with tungsten bronze structure has arisen as a new photocatalyst for water splitting and CO_2 reduction under UV light irradiation. $KCaSrTa_5O_{15}$ showed activity for water splitting without a cocatalyst. In addition, NiO was an effective cocatalyst. The NiO cocatalyst activated during water splitting was dark purple and possessed a Ni hydroxide-shell–NiO-core structure as an active site for water reduction. The apparent quantum yield of optimized NiO-loaded $KCaSrTa_5O_{15}$ was 2.3% at 254 nm for water splitting. On the other hand, the Ag-loaded $KCaSrTa_5O_{15}$ photocatalyst was active for CO_2 reduction to CO in an aqueous medium. The Ag cocatalyst activated during CO_2 reduction gave a surface plasmonic absorption band in the visible light region suggesting that fine metallic Ag particles are the active sites for CO_2 reduction. The isotope experiment using $^{13}CO_2$ revealed that the carbon source of produced CO was CO_2 molecules. Moreover, a stoichiometric amount of O_2 evolved and TON_{CO_2} calculated from products was larger than 1 indicating that CO_2 reduction to CO photocatalytically proceeded using water as an electron donor.

Acknowledgements

This work was supported by a Grant in Aid (No. 24246131) from the Ministry of Education, Sports, Science & Technology in Japan and the ENEOS hydrogen foundation.

References

1 J. Hawecker, J. M. Lehn and R. Ziessel, *J. Chem. Soc., Chem. Commun.*, 1983, 536.
2 J. Hawecker, J. M. Lehn and R. Ziessel, *Helv. Chim. Acta*, 1986, **69**, 1990.
3 H. Takeda, K. Koike, H. Inoue and O. Ishitani, *J. Am. Chem. Soc.*, 2008, **130**, 2023.
4 H. Takeda and O. Ishitani, *Coord. Chem. Rev.*, 2010, **254**, 346.
5 T. Yui, Y. Tamaki, K. Sekizawa and O. Ishitani, in *Photocatalysis, Top. Curr. Chem.*, ed. C. A. Bignozzi, Springer, 2011, vol. 303, pp. 151–184.
6 Y. Tamaki, K. Watanabe, K. Koike, H. Inoue, T. Morimoto and O. Ishitani, *Faraday Discuss.*, 2012, **155**, 115.
7 S. M. Aliwi and K. F. Al-Jubori, *Sol. Energy Mater.*, 1989, **18**, 223.
8 M. Kanemoto, K. Ishihara, Y. Wada, T. Sakata, H. Mori and S. Yanagida, *Chem. Lett.*, 1992, 835.
9 K. Koči, L. Obalova and Z. Lacny, *Chem. Pap.*, 2008, **62**, 1.
10 S. N. Habisreutinger, L. Schmidt-Mende and J. K. Stolarczyk, *Angew. Chem., Int. Ed.*, 2013, **52**, 7372.
11 M. Tahir and N. S. Amin, *Energy Convers. Manage.*, 2013, **76**, 194.
12 S. Navalon, A. Dhakshinamoorthy, M. Alvaro and H. Garcia, *ChemSusChem*, 2013, **6**, 562.
13 J. Mao, K. Li and T. Peng, *Catal. Sci. Technol.*, 2013, **3**, 2481.
14 K. Sayama and H. Arakawa, *J. Phys. Chem.*, 1993, **97**, 531.
15 K. Iizuka, T. Wato, Y. Miseki, K. Saito and A. Kudo, *J. Am. Chem. Soc.*, 2011, **133**, 20863.
16 K. Teramura, Z. Wang, S. Hosokawa, Y. Sakata and T. Tanaka, *Chem. – Eur. J.*, 2014, **20**, 9906.
17 A. Kudo and Y. Miseki, *Chem. Soc. Rev.*, 2009, **38**, 253.
18 H. Kato and A. Kudo, *Catal. Today*, 2003, **78**, 561.
19 A. Kudo, H. Okutomi and H. Kato, *Chem. Lett.*, 2000, 1212.
20 Y. Miseki, H. Kato and A. Kudo, *Energy Environ. Sci.*, 2009, **2**, 306.
21 D. Nelson, B. Scheetz and C. Abate, *The International Centre for Diffraction Data*, #40-351.
22 H. Kato and A. Kudo, *J. Phys. Chem. B*, 2001, **105**, 4285.
23 M. P. Seah, *Surf. Interface Anal.*, 1989, **14**, 488.
24 A. Iwase, H. Kato and A. Kudo, *Appl. Catal., B*, 2013, **89**, 136.
25 Y. Negishi, M. Mizuno, M. Hirayama, M. Omatoi, T. Takayama, A. Iwase and A. Kudo, *Nanoscale*, 2013, **5**, 7188.
26 Y. Hori, K. Kikuchi and S. Suzuki, *Chem. Lett.*, 1985, 1695.
27 Y. Hori, H. Wakebe, T. Tsukamoto and O. Koga, *Electrochim. Acta*, 1994, **39**, 1833.
28 T. Hatsukade, K. P. Kuhl, E. R. Cave, D. N Abram and T. F. Jaramillo, *Phys. Chem. Chem. Phys.*, 2014, **16**, 13814.
29 O. Ishitani, C. Inoue, Y. Suzuki and T. Ibusuki, *J. Photochem. Photobiol., A*, 1993, **72**, 269.
30 K. Domen, A. Kudo, T. Onishi, N. Kosugi and H. Kuroda, *J. Phys. Chem.*, 1986, **90**, 292.
31 Q. Jia, Y. Miseki, K. Saito, H. Kobayashi and A. Kudo, *Bull. Chem. Soc. Jpn.*, 2010, **83**, 1275.
32 H. Kato, K. Asakura and A. Kudo, *J. Am. Chem. Soc.*, 2003, **125**, 3082.
33 K. Matsubara and T. Tatsuma, *Adv. Mater.*, 2007, **19**, 2802.

